JOURNAL OF GEOPHYSICAL RESEARCH, VOL. 106, NO. B3, PAGES 4121–4128, MARCH 10, 2001

A proposed method for locating the critical region of a future earthquake using the critical earthquake concept

Wenzheng Yang

Center for Analysis and Prediction, China Seismological Bureau, Beijing, China

David Vere-Jones

Institute of Statistics and Operations Research, Victoria University of Wellington, Wellington, New Zealand

Ma Li

Center for Analysis and Prediction, China Seismological Bureau, Beijing, China

Abstract. Using the critical point concept and extending Bowman's idea of critical earthquake, we develop an intersecting circle method to locate the critical region. A simulation check shows that this method is effective in finding a given critical region. We selected several real cases from New Zealand and China and used this method to find the critical regions before the occurrence of large earthquakes. The result shows that this method is valid for detecting a critical region and the epicenter of mainshock might be in the critical region.

1. Introduction

Prior to some large earthquakes, investigators have found evidence that the region around the epicenter is in a stage of abnormality for a period of time during which the occurrence of middle-sized earthquakes accelerate [*Sykes and Jaumé*, 1990; *Triep and Sykes*, 1997]. *Knopoff et al.* [1996] pointed out that all 11 earthquakes in California with nominal magnitudes greater than or equal to 6.8 from 1941 to 1993 were preceded by an increase in the rate of occurrence of earthquakes having magnitude greater than 5.1. *Varnes* [1989] and *Bufe and Varnes* [1993] quantified this kind of phenomenon by putting forward the time-to-failure relation between cumulative moment release and time, and this relation is commonly shown in articles [*Gross and Rundle*, 1998; *Yang and Ma*, 1999; *Robinson*, 2000] with

$$\sum M(t)^{\alpha} = A + B(t_f - t)^{\beta}, \tag{1}$$

where $M(t)$ is the moment release as a function of time t, α, A, B, and β are constants, and a major earthquake is expected to occur at t_f. *Sornette et al.* [1995] add a log-periodic correction part to (1) with

$$\sum M(t)^{\alpha} = A + B(t_f - t)^{\beta}\left[1 + C\cos\left(2\pi\frac{\log(t_f - t)}{\log\lambda} + \Psi\right)\right], \tag{2}$$

where C, λ, and Ψ are new constants. The moment release is believed to increase exponentially with the size of the earthquake, and we follow the formulation of *Kagan* [1997] with

$$\log M = 1.5m + 9, \tag{3}$$

where m is the magnitude and M is the seismic moment in N m.

Paper number 2000JB900311.
0148-0227/01/2000JB900311$09.00

Equation (1) indicates that the regional moment release will accelerate until the occurrence of a large event. Thus those potential forecasting models using (1) or (2) can be categorized as accelerating moment release (AMR) model. *Bufe and Varnes* [1993] used (1) to retrospectively predict the time and magnitude of several large earthquakes that occurred in San Francisco Bay region. From then on, other instances of large earthquakes were tested with (1) or (2), but most of these studies had been conducted in plate boundary regions. *Yang and Ma* [1999] used this model to study several historical large earthquakes in China and found that 10 out of 15 cases had obviously accelerating moment release prior to mainshock.

In the beginning, crack propagation or other traditional theories were used to explain AMR model [*Bufe and Varnes*, 1993]. However, observational evidence (e.g., precursory events are so widely separated that it is unlikely that they are related mechanically; the apparent existence of a critical radius; an increase in event size with growing stress correlation length; the presence of a linear region and a scaling region in the cumulative moment release curve [*Sammis and Smith*, 1999]) drives more and more researchers to focus on the critical point hypothesis [*Main*, 1996; *Saleur et al.*, 1996; *Bowman et al.*, 1998; *Jaumé and Sykes*, 1999] and borrow some ideas from statistical physics. *Jaumé and Sykes* [1999] reviewed the use of AMR model for large and great earthquakes and found four major characteristics of this model that are consistent with the critical point hypothesis.

The concept of criticality in regional seismicity embodies more usable information than just power laws for precursory phenomena, which are only valid very near the critical point [*Saleur et al.*, 1996]. In a critical region, power law behavior plays an important role in governing the level of criticality and distinguishes the critical region from noncritical regions, where the seismicity rate is constant or decreasing. Assuming the critical region is to have the shape of a circle, *Bowman et al.* [1998] presented a method for finding the best estimate of

the size of the critical region by minimizing the error in fitting a power law to the data. After setting the epicenter of the large earthquake to be the center, they calculate the ratio of power law fit RMS (root-mean-square) error to linear fit RMS error in circles with different radii and then choose the circle in which the ratio is the lowest to represent the size of the critical region. In this way, they systematically analyze the seismicity of California and arrive at the empirical relation

$$\log R \propto Cm, \quad (4)$$

where R is the radius of the critical region associated with the occurrence of a large earthquake of magnitude m and C is constant. For the eight large events post-1950 in California and additional four events, *Bowman et al.* [1998] suggested C=0.44; *Brehm and Braile* [1998] conducted a similar study to analyze nineteen events from the New Madrid zone and found C=0.75; *Jaumé and Sykes* [1999] combined the two data sets and found C=0.36. However, given the magnitude of the earthquake, we can draw only limited information on how big the critical radius will be from (4), because the error bar in Figure 5 of *Jaumé and Sykes* [1999] has a wide range (e.g., if there exists a kind of accelerating moment release around the epicenter of a magnitude 7 event prior to its occurrence, the critical radius for it may vary in a wide range from 80 to 300 km).

Brehm and Braile [1999] proposed a mainshock search location technique, which used grid-scanning algorithm and a kind of normalized search radius to find future mainshock location. The method proposed in section 2 represents another attempt to extract additional information about the probable critical region of a forthcoming event from the background region using test regions with their centers on a given grid.

2. Method

Before the occurrence of a large earthquake, an anomalous region forms. As the critical point draws near, the radius of the critical region provides information on how large the forthcoming earthquake in it would be. If the mainshock only occurs within the critical region and the critical region is significantly different from its background, an interesting question arises: Could we use the concept of criticality to locate the epicenter of a forthcoming large earthquake? As we know, one of the characteristics of critical point hypothesis is the long-range correlation. How does the long-range correlation embody itself in space when system comes to the stage of criticality? If a large earthquake can be viewed as a critical point for some tectonic domain, then the observed increase in activity and long-range spatial correlation are expected precursory phenomena [*Saleur et al.*, 1996]. So, if the epicenter of mainshock is on or near to the critical point, there might exist some methods to detect the epicenter of the mainshock before its occurrence. *Bowman et al.* [1998] fixed the epicenter of a strong earthquake to be the center of the critical region and changed the radius of the circle in fixed steps. Among these concentric circles, the one in which the cumulative moment release curve was best fitted by power law was accepted as the critical region for the strong earthquake. However, before the occurrence of a large earthquake, nothing was known about the epicenter of mainshock, and no previous research was carried out relative to the behavior around points other than the epicenter. If we select a point that is near to the center of the critical region and do the same kind of routine as *Bowman et al.* [1998] did at the epicenter, it is reasonable to believe that the radius of the "critical region" (or critical circle) for the selected point will be larger than the critical radius for the center of the critical region and the critical region for the point will still cover the center, Because the critical region of a point that is away from the center of critical region has to include those events around the center so as to let its cumulative moment release curve be best fitted by the power law. Therefore, if we select a series of points around the epicenter, try to find the best "critical circle" for each of them, and then plot these circles on map, we will find that most of these circles have a tendency to cover the center of critical region. With this idea, we develop a grid-scanning algorithm to identify the location of the critical region; we put it forward as a possible way to locate the epicenter of a forthcoming large critical earthquake.

3. Simulation Check

A synthetic catalog was constructed as a background and for comparison, in which the distribution of magnitudes was controlled by the Gutenberg-Richter relationship with the b value equal to 1 and in which the spatial distribution was simulated from a homogeneous Poisson process. To construct a catalog governed by (1), we followed the simulative method of AMR model suggested by D. Vere-Jones et al. (Remark on accelerated moment release model for earthquake forecasting: problems of simulation and estimation, manuscript in preparation, 2000), using parameters similar to the Arthur's Pass earthquake (M6.7, 1994) in New Zealand. All routines used in this research were written in S-plus, with the aid of SSLib (Statistical Seismology Library) compiled by *Harte* [1999]. Equation (1) was used here to be the power law with α =0.5. The fitting function used in this study was nlmin() in S-plus, which can find a local minimum to a nonlinear function [*Dennis and Mei*, 1979]. The minimum number of events for fitting is 10.

Here we give a simplified introduction to a simulation method for the AMR model; for a more detailed description of this method we refer to D. Vere-Jones et al. (manuscript in preparation, 2000).

The usual approach in developing a stochastic model for a situation described in broad terms by a deterministic equation is to treat the approximating deterministic equation as relating to the expected value of the random quantity it purports to represent (D. Vere-Jones et al., manuscript in preparation, 2000). Let $S(t) = \sum M^{\alpha}(t)$, $B = -B$, $T = t_f - t_0$ (where t_0 is the begining time of cumulative moment release) and $\theta = \beta$, then (1) could be replaced by

$$E[S(t)] = A - B(T-t)^{\theta}, \quad (5)$$

and the expected increment over a short time interval *(t, t+dt)* can be written as

$$E[dS(t)] = E[\frac{dN(t)}{dt}]E[S \mid S \text{ occurs at } t], \quad (6)$$

where $E[{dN(t)}/{dt}]$ is the expected number of events occurring in *(t, t+dt)*, and $E[S \mid S$ occurs at $t]$ is the expected mean event size occurring in *(t, t+dt)*. If we let $E[{dN(t)}/{dt}]=\lambda(t)$ and $E[S \mid S$ occurs at $t]=\mu(t)$, then we get

$$\mu(t)\lambda(t) = B\theta(T-t)^{\theta-1}. \quad (7)$$

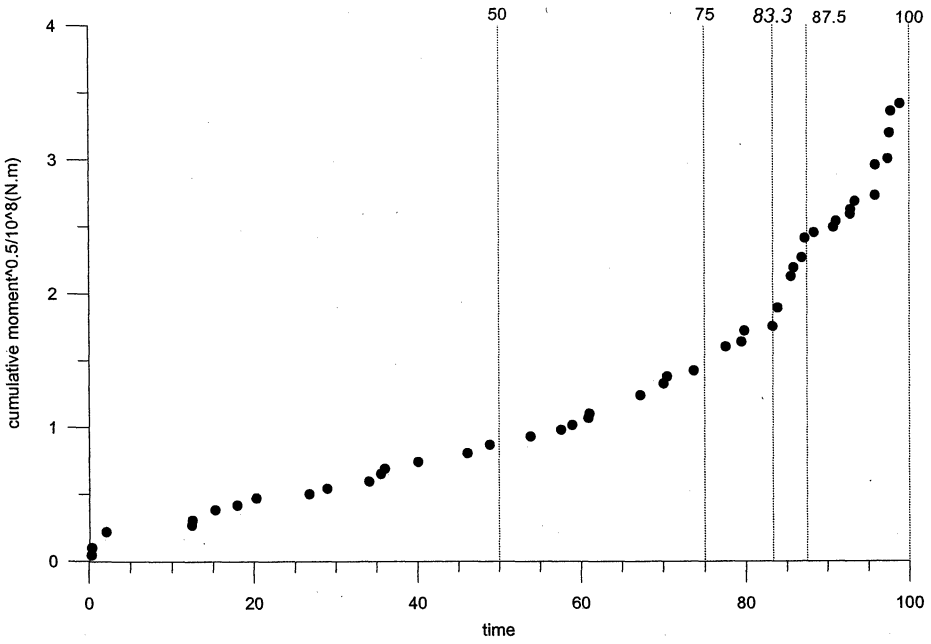

Figure 1. A plot of simulated cumulative moment release curve, in which the data were generated by AMR model. The curve could be divided into linear region and scaling region at $5/6T$=$0.833T$, when T is the total estimated time to the large event. Each number on the top of vertical line shows its time point.

Here we arbitrarily treat

$$\mu(t) = H(1-\frac{t}{T})^{q(\theta-1)} \tag{8a}$$

$$\lambda(t) = G(1-\frac{t}{T})^{p(\theta-1)}, \tag{8b}$$

where p, q, H, G are constants. $0 \le p,\ q \le 1$ and $p+q=1$. Specially, if $q=0$, then the cumulative moment release is equal to cumulative number release, G is the total number in $(0, T)$. Generally, we can take $p=q=0.5$, but several cases show that the frequency part should take a larger proportion of the total cumulative moment release than the size part [e.g., *Knopoff et al.*, 1996]. With (8a) and (8b), the stage of simulation could be finished with standard methods for point processes (e.g., the thinning method). The simulation of $\mu(t)$ needs the use of the Kagan distribution (D. Vere-Jones et al., manuscript in preparation, 2000), which is a refinement of the Gutenberg-Richter distribution used for dealing with large events.

For our simulation check here, we first made a synthetic catalog with random (Poisson) events distributed over an area of $10^\circ \times 10^\circ$. 998 earthquakes occurred in this region over a time interval of 100 time units. The magnitude cutoff is 4.0. All (46 events) earthquakes that fell within the circle, radius 200 km and center (5°, 5°), were selected and replaced by the same number of earthquakes generated by the AMR model. Thus this catalog contained both events from a critical region (with accelerating moment release) and noncritical regions (containing random events). We also kept the original catalog, which contained no critical region, for comparison while several tests were carried out on both catalogs. The points of a 10×10 spatial grid were taken as potential critical points, and the procedure outlined above was used for each point to find the best radius for the power law cumulative moment release curve. The circle with the best radius for each point was then drawn. The radii varied from 10 to 800 km. In addition, a second 20×20 spatial grid was constructed, and the number of circles covering each grid point was counted. The density of the circle-covering grid should be higher than that of the critical circle-searching grid, so as to ensure the contour map of the critical regions has a reasonable accuracy.

Figure 1 shows one series of cumulative moment release data with 46 events generated by AMR model for the critical region. We can see that the data could be divided into two parts (linear region and scaling region) at the time point near $5/6T$=83.33 based on different slopes. In order to show the dynamic process of evolving toward the critical stage, we made five synthetic catalogs in which the critical regions were at the time stage of 0, $0.5T$, $0.75T$, $0.875T$, and T respectively, and the events in the noncritical region were the same for all of these stages. The total number of events in the critical region was 46 and the time length was 100 time units for all of these stages. The last four stages corresponded with the vertical lines in Figure 1. At the time stage of T, a mainshock was expected to occur at T, and we set the end time a little before T, so as not to include the mainshock. For the contour maps in Figure 2, at the time stage of zero, there is no critical region, all events are distributed homogeneously in space, and the high contour value region is dispersed with low absolute value. When the stage evolves to $0.5T$, there exists an obvious high value region of intersecting circles, but it is to the northeast of the center of the critical region and covers a small area. For the stage at $0.75T$, which is still in the linear period, the high value region seems to be weakened and scattered. When the stage is at $0.875T$, which is in the scaling period and the high value region is strengthened and centralized again. The high value region also includes the center of the critical region, although both centers do not coincide. When the stage evolves to T, the center of the high value region coincides with the center of the critical region, and the shape of the high value region is more circular. From Figure 2 we can find that the precursory phenomenon of accelerating moment release to the critical point exists very early (at least begins at $0.5T$), but it is so unstable and

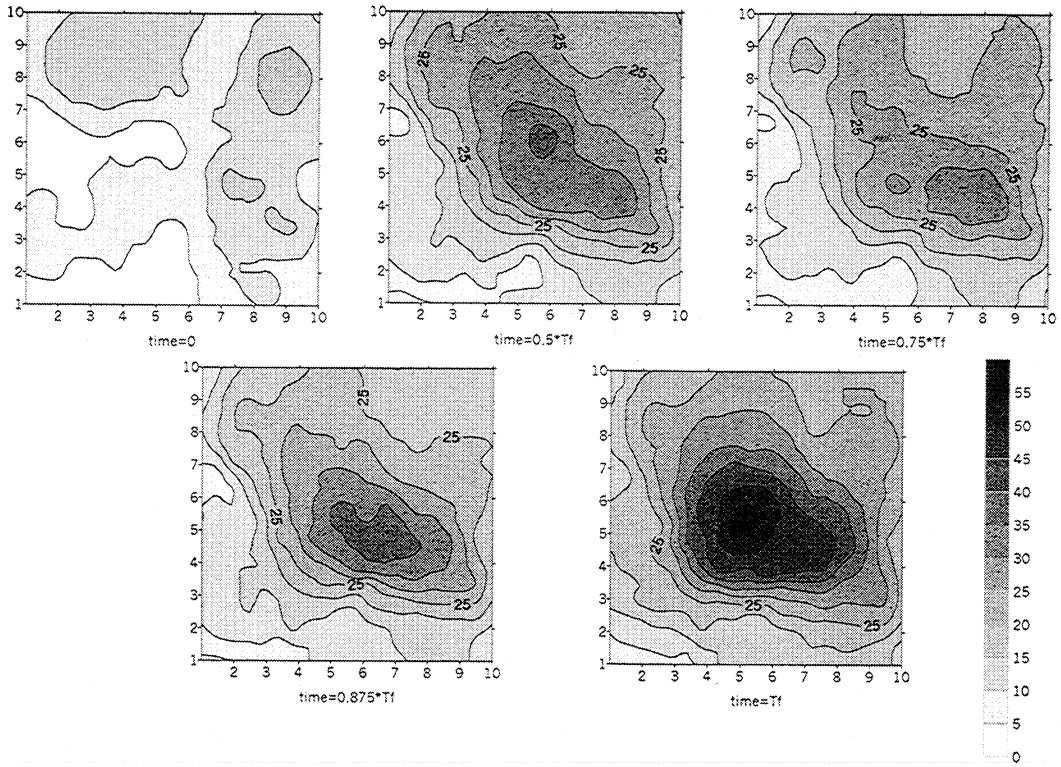

Figure 2. Plots of 998 earthquakes generated to be distributed in $10^\circ \times 10^\circ$ area with a time period from 0 to 100 time units. The critical region is defined to be the circle with radius 200 km and center (5°, 5°). The intersecting circle method is used to detect the evolving critical region at five time stages (0, $0.5T$, $0.75T$, $0.875T$, and T). The results are illustrated with a contour map. The value of scale means how many circles cover a point.

ephemeral that we cannot find the location of the critical region until it evolves toward criticality during the scaling period. In the scaling region, the high value region becomes broader and higher as time moves to T, and the centers of the high value region and the critical region coincide with each other.

4. Applications

In this section, we test this method on several large earthquakes that occurred in New Zealand and in northwest China after 1970. Because we use relatively high magnitude cutoff (4.5 for the case of New Zealand and 4.0 for the case of China) and the magnitude computation methodologies have been consistent since 1970, we believe that the man-made catalog inhomogeneities and aftershocks could only play a minor role in the results. The simulations of *Gross and Rundle* [1998] suggest that the time-to-failure technique is robust enough to apply to catalogs with magnitude uncertainties of several tenths of a unit. Therefore we kept the original catalogs and did not adjust the magnitudes or delete aftershocks.

4.1. Application to the Arthur's Pass Earthquake

The Arthur's Pass earthquake occurred in New Zealand on June 18, 1994, 43.01°S, 171.46°E, with magnitude 6.7, and was the largest of a regional cluster of moderate magnitude events in the central South Island, from 1984 through 1995 [*Robinson*, 1997].

The catalog used in this study was provided by *Robinson* [1997] with a magnitude threshold of 4.5 and only includes those events with depths of 40 km or less [*Robinson*, 2000]. Table 1 lists three events with magnitude larger than 6.5 after 1990 in this catalog. In discussing large earthquakes in California, *Knopoff et al.* [1996] pointed out that the precursors to a strong earthquake might appear over a time interval of the order of 5 to 10 years before the strong earthquake. Here we used the data from 1970 to 1993. The end time of the study was set to August 1, 1993, so as to avoid including any of the three large earthquakes in the catalog.

The seismic region of New Zealand is a narrow belt in the NE direction. Sixteen points from NE to SW in a line were selected with equal distance as centers of possible critical regions. The location of the first point is 37°S 180°E and the location of the last point is 47°S 165°E. For each center, the best radius was determined by the method described earlier, and the numbers of circles covering the points of a second grid were counted. Figure 3 shows the distribution of the 16

Table 1. Earthquakes ($M_L \geq 6.5$) from 1980 to 1997 in New Zealand

Date	Longitude	Latitude	Magnitude
Aug. 10, 1993	166.71	-45.21	6.7
June 18, 1994	171.46	-43.01	6.7
Feb. 5, 1995	179.49	-37.65	7.0

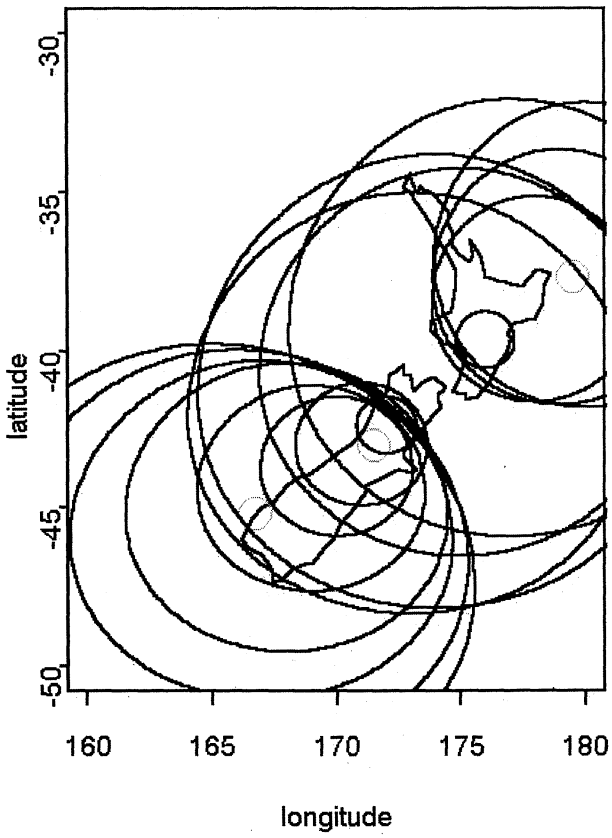

Figure 3. Sixteen critical circles along NE-SW direction in New Zealand. Three little thin circles represent the epicenters of earthquakes which occurred after August 1, 1993, and larger than 6.5.

circles. Figure 4 shows that the most covered area is near to the epicenter of Arthur's Pass earthquake. However, this method did not find any obvious critical regions for the remaining two large earthquakes in Table 1. One possible explanation might be that both of the two remaining earthquakes occurred in the sea off the two ends of New Zealand, and their long time foreshocks might be incomplete for this method to detect accelerating moment release. Another reason may be that few potential centers were selected in the sea off the two ends of New Zealand.

In a later work, we set the magnitude cutoff to be 5.0, and the result was similar to that of 4.5. We also shifted the line of possible critical centers 0.5° north or west, and no obvious difference was found. We extended the line of the possible critical centers to cover the two large events in both edges of New Zealand, and three critical regions were found on the contour map. The epicenter of the Arthur's Pass earthquake was right in the center of the middle one, but the epicenter of the East Cape (M7.1, 1995) earthquake was nearly 200 km SSW of its critical center, and the epicenter of the Secretary Island (M6.7, 1993) earthquake was nearly 400 km NNE of its critical center.

4.2. Application to Earthquakes in the South Tianshan Region

The South Tianshan region (Figure 5) passes through the western edge of China and has a high frequency of earthquake occurrence. For this work, a catalog compiled by Seismological Bureau of Xinjiang Uygur Autonomous Region was used. This covers the South Tianshan region from 1970 to 1999 with a magnitude threshold of 4.0. Five time intervals were selected, based on the magnitude-time plot between January 1, 1970, and April 10, 1999 (Figure 6). No earthquake larger than 6.5 occurred in any of the five intervals, while the overall list of catalog events with magnitudes equal to or larger than 6.5 are shown in Table 2. The beginning of each time interval was taken to be just after the occurrence of the last event with magnitude larger than 6.5 in the region.

A 10×10 grid was taken in the rectangle with corners (37°N, 73°E), (37°N, 80°E), (42°N, 73°E), (42°N, 80°E), and the grid points used as centers of potential critical regions. As in the previous examples, a second grid was then used to count the numbers of covering circles. The first interval began on January 1, 1970, and ended on August 10, 1974, with the occurrence of the Wuqia earthquake one day later. As shown in Figure 7a, the Wuqia earthquake with magnitude 7.3 occurred inside the region with the highest number (26) of intersecting circles. The end time of interval 2 was set on February 12, 1983, one day before the Wuqia M6.7 earthquake occurred. This earthquake and the subsequent magnitude M7.1 earthquake on August 23, 1985, both occurred near the peak value for the number of intersecting circles. A third large earthquake with magnitude 7.1 occurred on July 29, 1985, but lay outside the region of high values (see Figure 7b). We did not try to calculate the result of interval 3 because it was too short. Interval 4 ranged from July 5, 1991, to March 18, 1996, one day before the Atushi M6.9 earthquake, which again occurred near the peak values for the numbers of intersecting circles (see Figure 7c). Interval 5 began after the Atushi M6.9 earthquake, March 19, 1996, but no large earthquake has yet occurred in the region of study after this date. The peak value moves a little north, as shown in Figure 7d. From Figures 7a to 7d, we can see that the peak value moves as time goes by, from west to northeast, but this is an obvious conclusion because the locations of the large earthquake, themselves move from west to northeast also.

5. Discussion

If the critical point hypothesis is accepted, the preceding shocks and the following mainshock should be correlated in space and time. In the time domain the frequency and magnitude of preceding shocks should increase as the time of the mainshock approaches. In the space domain, different sizes of mainshocks should have different critical radii, and the larger the magnitude, the larger the radius. We would then expect a property of the critical earthquake radius is that the cumulative moment release of foreshocks in the circle would be fitted best by a power law, whereas the cumulative moment release curve in a noncritical region would be more like a straight line. The critical region also experiences background earthquake activity, and the behavior of the long-range correlation will be obvious and strong when the region evolves to criticality. For those points that are not close to the center of critical region, the critical radius would be reached until the circle is large enough to cover the center of the critical region. Using this idea, an intersecting circle method was developed to find the center of the critical region, in anticipation that the epicenter of the future mainshock would not be far from the center of the critical region so obtained.

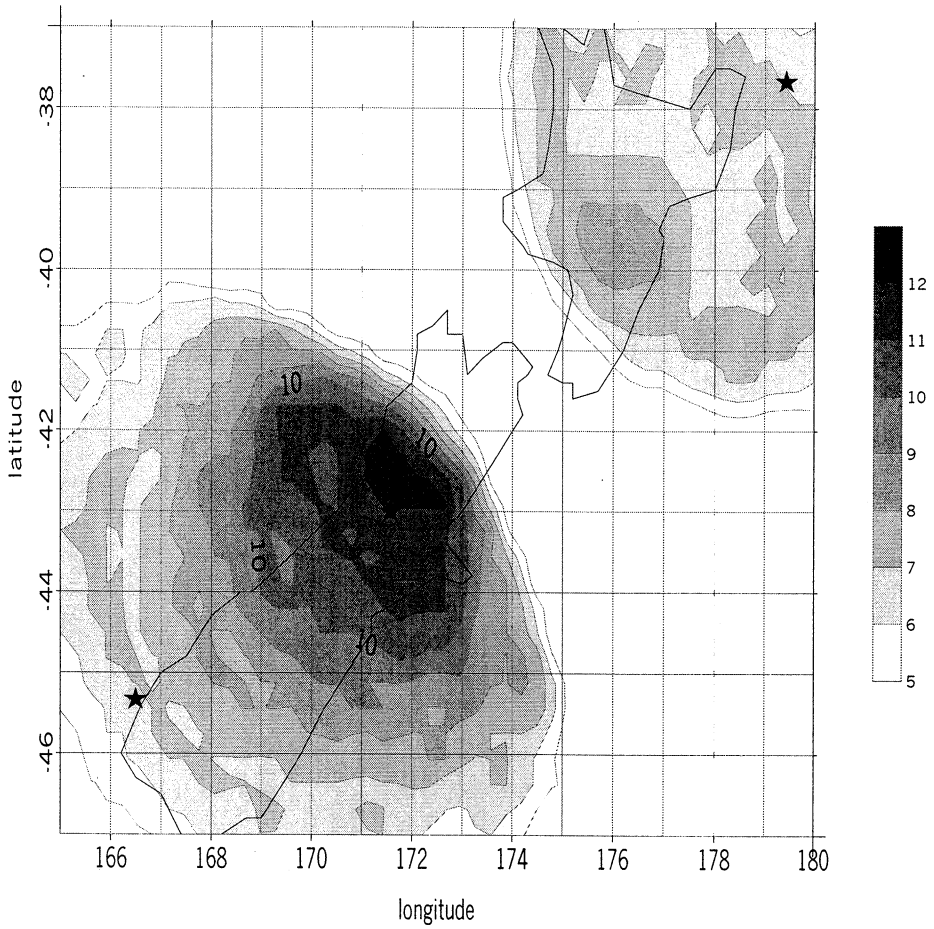

Figure 4. Contour map of Figure 3. The star in the middle shows the Arthur's Pass earthquake (M6.7, 1994). The star to the south edge is the Secretary Island earthquake (M6.7, 1994), and the star to the north edge is the East Cape earthquake (M7.0, 1995).

A simulation check using a simplified model for accelerated moment release behavior suggests that this method should be capable of detecting the critical region at several stages of the evolving critical process. Some indications of criticality may exist as early as $0.5T$, but the center of critical region could not be located until it evolves to the scaling region, which begins at nearly $0.833T$.

A check of the New Zealand catalog with a one-dimensional grid prior to three recent large earthquakes shows that this method is able to find the critical region for the Arthur's Pass earthquake. However, when applied to the two remaining earthquakes that lay at the two edges of New Zealand, this method did not give good results for their critical regions. We think the reasons are that too few potential critical points were selected for them and their long

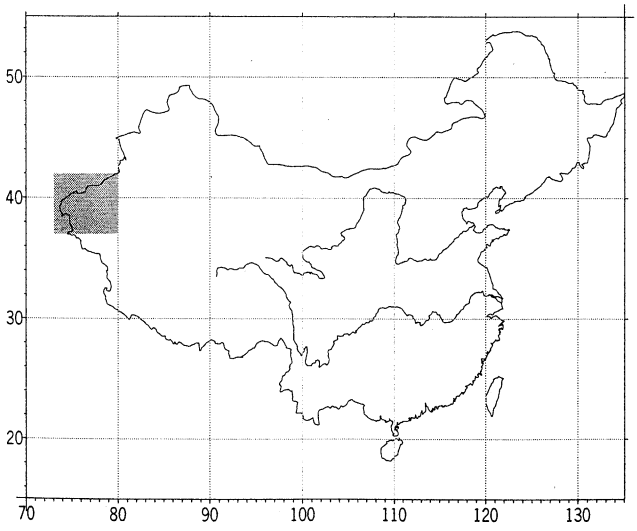

Figure 5. The location of study region (rectangular shade) on the map of China

Table 2. Earthquakes ($M \geq 6.5$) from 1970 to 1997 in South Tianshan

Date	Longitude	Latitude	Magnitude
Aug. 11, 1974	73.83	39.23	7.3
Feb. 13, 1983	75.23	40.23	6.7
July 29, 1985	73.80	37.20	7.1[a]
Aug. 23, 1985	75.48	39.43	7.1
Sept. 12, 1985	75.45	39.43	6.6[b]
March 25, 1990	73.18	37.18	6.7[a]
Feb. 25, 1991	79.00	40.33	6.5
July 14, 1991	73.25	37.48	6.5[a]
March 19, 1996	76.63	40.13	6.9

[a] Events occurred outside of China.

[b] Aftershock of the M7.1 event above it.

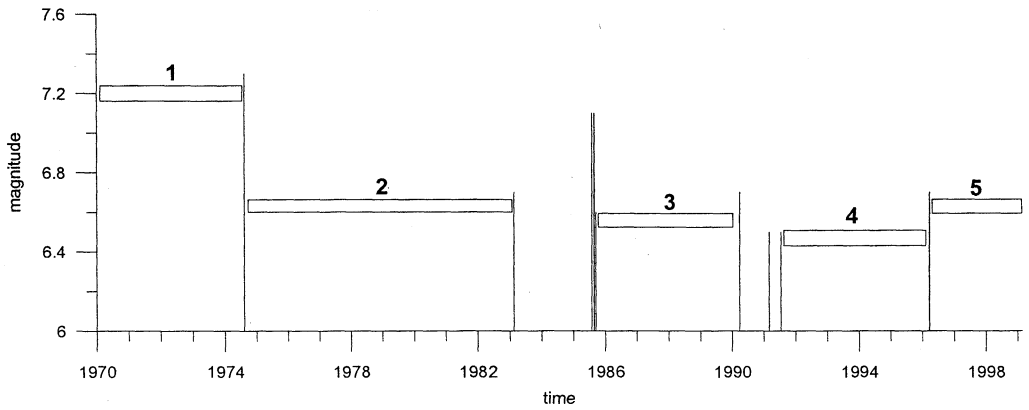

Figure 6. The magnitude-time plot of events with $M \geq 6.5$ in South Tianshan region (37°N~42°N, 73°E~80°E) from January 1, 1970 to April 10, 1999. Five time intervals were selected based on time intervals of earthquakes with $M \geq 6.5$, and four of them were studied in this article.

time foreshocks might be incomplete for this method to detect accelerating moment release.

Because of the high seismicity in the South Tianshan region, we were able to use the intersecting circle method with a two-dimensional grid to study the seismicity of this area during several time periods. The results show that out of nine earthquakes larger than 6.5, four of them lie near to the centers of critical regions, and of the remaining five

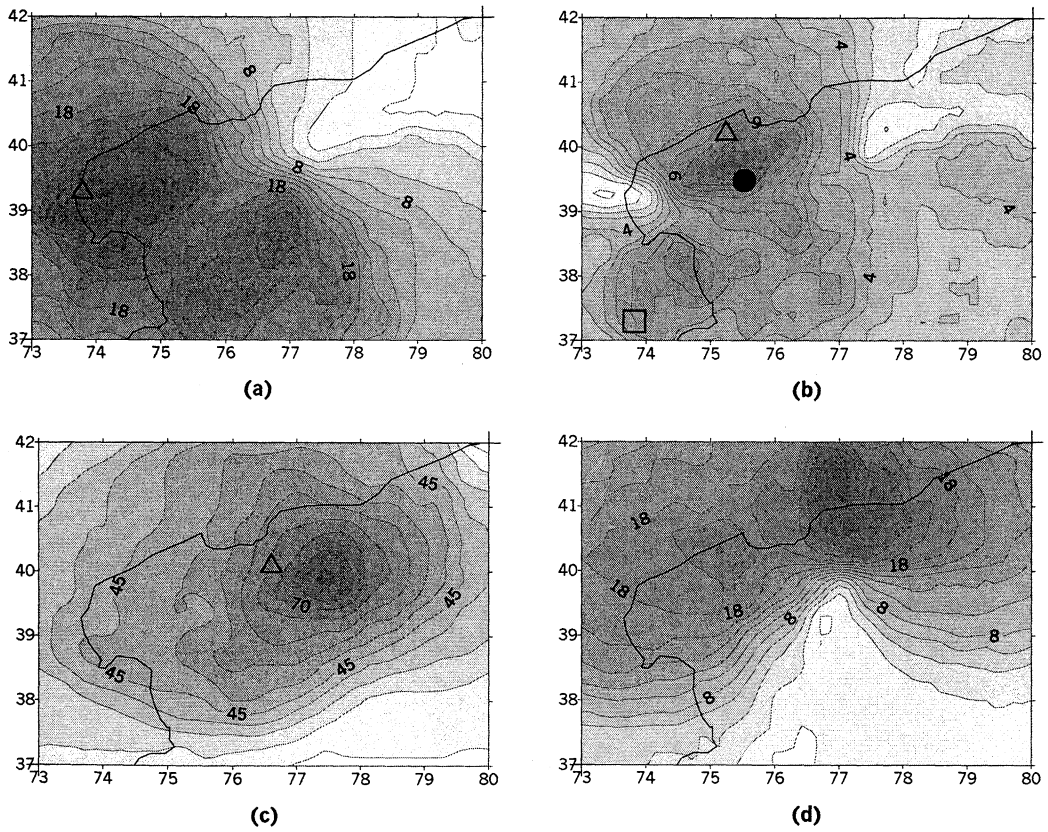

Figure 7. The contour maps obtained by applying the intersecting circle method to four time intervals in South Tianshan region. In Figure 7a, the time interval begins at January 1, 1970, and ends at August 10, 1974. The triangle shows the epicenter of Wuqia $M7.3$ (August 11, 1974) earthquake. In Figure 7b, the time interval begins at August 13, 1974, and ends at June 22, 1981. The triangle shows the epicenter of the Wuqia $M6.7$ (February 13, 1983) earthquake, the solid circle shows the epicenter of the Wuqia $M7.1$ (August 23, 1985) earthquake, and the rectangle shows the epicenter of $M7.1$ (July 29, 1985) earthquake. In Figure 7c, the time interval begins at July 15, 1991, and ends at March 19, 1996. The triangle shows epicenter of Atushi $M6.9$ (March, 19, 1996) earthquake. In Figure 7d, the time interval begins at March 20, 1996, and ends at April 19, 1999. No earthquake larger than $M6.5$ has occurred in South Tianshan region since.

earthquakes, four of them lie outside of China. At this stage, this method is not effective to detect the critical region for those earthquakes lying near to the border.

It is hard to give a quantitative rule for determining how large the critical region is from the contour map directly. Although equation (4) shows a positive relation between critical radius and magnitude, the critical radii vary a lot between different earthquakes of the same magnitude. The absolute value of the contour is of little help in determining the size of the critical region without considering the background value. An empirical relation between the contour value and the range of critical region could be the ratio

$$\rho = \frac{\nu_c - \bar{\nu}}{\bar{\nu}}, \qquad (9)$$

where ν_c is the absolute value of contour map which represents the number of circles that cover a point in the map and $\bar{\nu}$ is the average value of ν_c. From all the contour maps available in this work, we find that the value of ρ in the range of 0.8 to 1.0 usually represents the region of criticality.

From the successful applications, we find that the epicenters of the mainshocks were not usually at the centers of their critical regions. For example, the epicenter of the Arthur's Pass earthquake was at the south edge of the highest contour value region in Figure 4. Figures 7a, 7b, and 7c show similar things also. The errors in the catalog and data processing might account for some of this departure. However, analogies with a sandpile model also suggest that a mainshock is likely to be more effective in moving a system away from criticality when it occurs near the edge of a critical region, than when it occurs near the center of the critical region.

Brehm and Braile [1999] treats a similar problem with somewhat related techniques like ours. However, the main differences lie in the methods used for assessing the potentiality of successive grid points as sites for future earthquakes. *Brehm and Braile* [1999] defined a parameter normalized search radius (NSR) and designated the region within the optimum search radius (the same as Bowman's critical radius) surrounding the point corresponding to the local maximum NSR value as the location of the mainshock. The method we have proposed rests on simpler assumptions. We believe that the critical circle of point in the neighborhood of mainshock's epicenter has a tendency to cover it.

In conclusion, this method is developed using the concept of critical point hypothesis and extending Bowman's idea on critical earthquake, and it is a potential method to locate future critical region. It will only be effective if the record of preceding shocks around the center of the critical region is accurate and complete.

Acknowledgments. We are grateful to Russell Robinson for valuable discussions during the course of this study and for providing the catalog of New Zealand for this research. David Harte suggested a good tool for the work of fitting. We thank Liu Jie and Shi Yaolin for their valuable suggestions. We appreciate the constructive comments of David Rhoades and two anonymous referees on an earlier version of the paper. We thank Charles Bufe for reviewing this manuscript and providing valuable suggestions. This study was sponsored by the Chinese Joint Seismological Science Foundation (198044), the New Zealand Asia 2000 Foundation and the Institute of Geological and Nuclear Sciences in New Zealand.

References

Bowman, D. D., G. Ouillon, C. G. Sammis, A. Sornette, and D. Sornette, An observational test of the critical earthquake concept, *J. Geophys. Res.*, *103*, 24,359-24,372, 1998.

Brehm, D. J., and L. W. Braile, Intermediate-term earthquake prediction using precursory events in the New Madrid Seismic Zone, *Bull. Seismol. Soc. Am.*, *88*, 564-580, 1998.

Brehm, D. J., and L. W. Braile, Intermediate-term earthquake prediction using the modified time-to-failure method in southern California, *Bull. Seismol. Soc. Am.*, *89*, 275-293, 1999.

Bufe, C. G., and D. J. Varnes, Predictive modelling of the seismic cycle of the greater San Francisco Bay region, *J. Geophys. Res.*, *98*, 9871-9883, 1993.

Dennis, J. E., and H. H. W. Mei, Two new unconstrained optimization algorithms which use function and gradient values, *J. Optimization Theory Appl.*, *28*, 453-483, 1979.

Gross, S., and J. Rundle, A systematic test of time-to-failure analysis, *Geophys. J. Int.*, *133*, 57-64, 1998.

Harte, D., Documentation for the Statistical Seismology Library, *Res. Rep. 98-10*, Sch. of Math. and Comput. Sci., Victoria Univ. of Wellington, Wellington, New Zealand, 1999.

Jaumé, S. C., and L. R. Sykes, Evolving towards a critical point: a review of accelerating seismic moment/energy release prior to large and great earthquake, *Prue Appl. Geophys.*, *155*, 279-306, 1999.

Kagan, Y. Y., Seismic moment-frequency relation for shallow earthquake: Regional comparison, *J. Geophys. Res.*, *102*, 2835-2852, 1997.

Knopoff, L., T. Levshina, V. I. Keilis-Borok, and C. Mattoni, Increases long-range intermediate-magnitude earthquake activity prior to strong earthquakes in California, *J. Geophys. Res.*, *101*, 5779-5796, 1996.

Main, I. G., Statistical physics, seismogenesis, and seismic hazard, *Rev. Geophys.*, *34*, 433-462, 1996.

Robinson, R., Recent New Zealand seismicity and models of accelerating precursory activity, *Sci. Rep. 97/27*, Inst. of Geol. and Nucl. Sci., Wellington, New Zealand, 1997.

Robinson, R., A test of the precursory accelerating moment release model on some recent New Zealand earthquakes, *Geophys. J. Int.*, *140*, 568-576, 2000.

Saleur, H., C. G. Sammis and D. Sornette, Discrete scale invariance, complex fractal dimensions, and log-periodic fluctuations in seismicity, *J. Geophys. Res.*, *101*, 17,661-17,677, 1996.

Sammis, C. G., and S. W. Smith, Seismic cycles and the evolution of stress correlation in cellular automaton models of finite fault networks, *Pure Appl. Geophys.*, *155*, 307-334, 1999.

Sornette, D., and C. G. Sammis, Complex critical exponents from renormalization group theory of earthquake: implication for earthquake predictions, *J. Phys. I France*, *5*, 607-619, 1995.

Sykes, L. R., and S. C. Jaumé, Seismic activity on neighboring faults as a long-term precursor to large earthquake in the San Francisco Bay area, *Nature, 348*, 595-599, 1990.

Triep, E. G., and L. R. Sykes, Frequency of occurrence of moderate to great earthquakes in intracontinental regions: Implications for change in stress, earthquake prediction, and hazards assessments, *J. Geophys. Res., 102*, 9923-9948, 1997.

Varnes, D. J., Predicting earthquakes by analyzing accelerating precursory seismic activity, *Pure Appl. Geophys.*, *130*, 661-686, 1989.

Yang, W., and L. Ma, Seismicity acceleration model and its application to several earthquake regions in China, *Acta Seismol. Sini.*, *12*, 35-45, 1999.

L. Ma and W. Yang, Center for Analysis and Prediction, China Seismological Bureau, PO Box 166, Beijing, 100036, China. (mali@sdb.ac.cn; ywz@seis.a.cn.)

D. Vere-Jones, Institute of Statistics and Operations Research, Victoria University of Wellington, PO Box 600, Wellington, New Zealand. (David.Vere-Jones@mcs.vuw.ac.nz)

(Received January 28, 2000; revised July 3, 2000;
accepted August 14, 2000.)